

# Optical Properties and Applications of Silicon Carbide in Astrophysics

Karly M. Pitman<sup>1</sup>, Angela K. Speck<sup>2</sup>,  
Anne M. Hofmeister<sup>3</sup> and Adrian B. Corman<sup>3</sup>

<sup>1</sup>*Planetary Science Institute*

<sup>2</sup>*Dept. of Physics & Astronomy, University of Missouri-Columbia*

<sup>3</sup>*Dept. of Earth & Planetary Sciences, Washington University in St. Louis  
USA*

## 1. Introduction

Optical properties, namely, spectra and optical functions, of silicon carbide (SiC) have been of great interest to astrophysicists since SiC was first theoretically posited to exist as dust, i.e., submicron-sized solid state particles, in carbon-rich circumstellar regions (Gilman, 1969; Friedemann, 1969). The prediction that SiC in space should re-emit absorbed radiation as a spectral feature in the  $\lambda = 10\text{-}13\ \mu\text{m}$  wavelength region (Gilra, 1971, 1972) was confirmed by a broad emission feature at  $\lambda \sim 11.4\ \mu\text{m}$  in the spectra of several carbon-rich stars (Hackwell, 1972; Treffers & Cohen, 1974). Many carbon-rich, evolved stars exhibit the  $\lambda \sim 11\ \mu\text{m}$  feature in emission, and SiC is now believed to be a significant constituent around them (Speck, 1998; Speck et al., 2009 and references therein).

### 1.1 Role of SiC in stellar environments

Detection of SiC in space provides much information on circumstellar environments because the chemical composition and structure of dust in space is correlated with, e.g., the pressure, temperature, and ratios of available elements in gas around stars. The mere presence of SiC implies that the carbon-to-oxygen (C/O) must be high. Different polytypes of SiC identify the temperature and gas pressure within the dust forming region around a star. The significance of SiC in stars is tied intimately to stellar evolution, as dust grains participate in feedback relationships between stars and their circumstellar envelopes that affect mass-loss rates, i.e., stellar lifetimes. Meteoritic SiC grains exhibit signatures of s-process enrichment, one of the main attributes of the evolutionary track of carbon-rich stars.

#### 1.1.1 S-process isotopic signatures in SiC

Elements more massive than helium have been formed in stars. All elements  $> {}^{56}\text{Fe}$  are generated by neutron capture because there is no Coulomb barrier for adding a neutral particle. In the s-process (slow neutron capture), neutrons are added to atomic nuclei slowly as compared to the rate of beta decay (cf. Burbidge, et al. 1957, a.k.a., B<sup>2</sup>FH; Cameron 1957). The precise isotopes of heavy elements depend on the rate of neutron capture, which, in turn, is strongly dependent on the properties of the stellar sources. Thus, it is possible to

uniquely identify different masses or types of stars as the sources of isotopically non-solar dust grains. SiC was the first meteoritic dust grain to be discovered that, on the basis of its isotopic composition, obviously formed before and survived the formation of the solar system (Bernatowicz et al., 1987). Further studies of the precise isotopic compositions of these meteoritic “presolar” grains have identified their stellar sources. For SiC, 99% of the presolar grains are characterized by high abundances of s-process elements, indicative of formation around certain classes of evolved, intermediate mass stars (described below).

### 1.1.2 Space environments containing SiC

Figure 1 illustrates the varied space environments in which SiC has been detected. To understand the nature of SiC in these environments and how SiC originally formed in the universe, Figure 2 and the following text describe how these categories of stars evolve.

#### 1.1.2.1 Asymptotic Giant Branch (AGB) stars

Figure 2 illustrates the evolution of low-to-intermediate-mass stars (LIMS; 0.8-8 times the mass of the Sun,  $M_{\odot} = 1.98892 \times 10^{30}$  kg). In the late stages of evolution, LIMS follow a path up the Asymptotic Giant Branch (AGB; Iben & Renzini, 1983). During the AGB phase, stars are very luminous ( $\sim 10^3$ - $10^4 L_{\odot}$ , where  $L_{\odot} = 3.839 \times 10^{33}$  erg/s) and large ( $\sim 300 R_{\odot}$ , where  $R_{\odot} = 6.995 \times 10^8$  m) but have relatively low surface temperature ( $\sim 3000$  K). AGB stars pulsate due to dynamical instabilities, leading to intensive mass loss and the formation of circumstellar shells of gas and dust. The carbon-to-oxygen ratio (C/O) controls the chemistry around the star: whichever element is less abundant will be entirely locked into CO molecules, leaving the more abundant element to control dust formation. Therefore, AGB stars can be either oxygen-rich or carbon-rich. Approximately 1/3 of AGB stars are C-rich (i.e., C/O > 1). Whereas C-stars are expected to have circumstellar shells dominated by amorphous or graphitic carbon, SiC is also expected to form; its IR spectrum provides a diagnostic tool not available from the carbonaceous grains. Therefore, SiC has been of greatest interest to astrophysicists seeking to understand the evolution of dust shells and infrared features of C-stars (Baron et al., 1987; Chan & Kwok, 1990; Goebel et al., 1995; Speck et al., 1997; Sloan et al., 1998; Speck et al., 2005, 2006; Thompson et al., 2006). For Galactic sources, the majority of C-stars should first condense TiC, then C, then SiC, as supported by meteoritic evidence (e.g., Bernatowicz et al., 2005). As C-stars evolve, mass loss is expected to increase. Consequently, their circumstellar shells become progressively more optically thick, and eventually the central star is obscured. Volk et al. (1992, 2000) christened such stars “extreme carbon stars” (e.g., Fig. 1a). Extreme carbon stars are expected to represent that small subset of C-rich AGB stars just prior to leaving the AGB. Because that phase is short-lived, the number of extreme C-stars is intrinsically small and few of these objects have been found in space ( $\sim 30$  known in the Galaxy: Volk et al., 1992, versus  $\sim 30,000$  known visible C-stars: Skrutskie et al., 2001).

#### 1.1.2.2 Post-AGB stars

Once the AGB phase ends, mass loss virtually stops, and the circumstellar shell begins to drift away from the star. At the same time, the central star begins to shrink and heat up from  $T = 3000$  K until it is hot enough to ionize the surrounding gas, at which point the object becomes a planetary nebula (PN; e.g., Fig. 1c). The short-lived post-AGB phase, as the star evolves toward the PN phase, is also known as the proto- or pre-planetary nebula (PPN) phase (e.g., Fig. 1b). As the detached dust shell drifts away from the central star, the dust cools, causing a PPN to have cool infrared colors. Meanwhile, the optical depth of the dust shell decreases,

allowing the central star to be seen and making such objects optically bright. The effect of decreasing optical depth and cooling dust temperatures changes the appearance of the circumstellar envelope, revealing features that were hidden during the AGB phase.

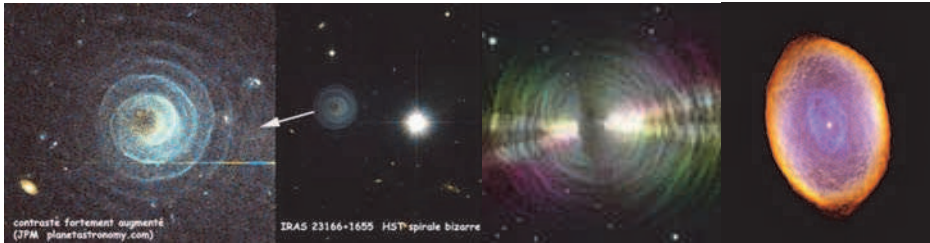


Fig. 1. Astronomical objects in which SiC has been detected. Left to right: (a) Hubble Space Telescope image of the extreme carbon star AFGL 3068. Source: Mauron & Huggins (2006); <http://www.planetastronomy.com> (b) The Egg Nebula, illustrating polarization through a thick vertical dust belt in the center of a pre- or proto-planetary nebula. Source: NASA and The Hubble Heritage Team (STScI/AURA); W. Sparks (STScI), R. Sahai (JPL); <http://heritage.stsci.edu> (c) IC 418, the Spirograph Nebula, is one of only a handful of galactic planetary nebulae that actually show SiC emission. Source: NASA and The Hubble Heritage Team (STScI/AURA); R. Sahai (JPL), A. Hajian (USNO); <http://hubblesite.org>

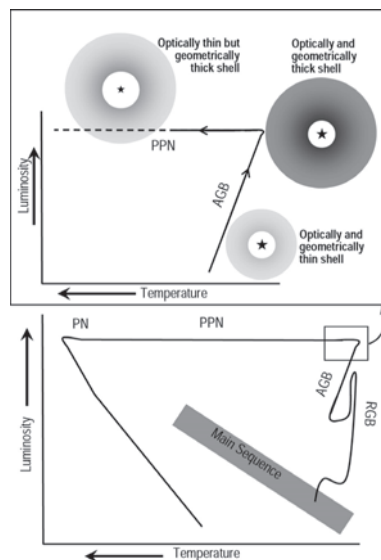


Fig. 2. Schematic diagram of the evolution of low-to-intermediate-mass stars. Bottom: A  $1M_{\odot}$  star begins its life on the main sequence, converting H into He in its core; when H is depleted, it exits to the Red Giant Branch (RGB), then the Asymptotic Giant Branch (AGB), where SiC formation occurs. Top: During the AGB phase, the dust shell get thicker and stars become very bright in the IR. Intense mass loss depletes the remaining H in the star's outer envelope in a few  $\times 10^4$  years (Volk et al., 2000) and terminates the AGB phase. Stars may then become proto-planetary nebulae (PPN), or later planetary nebulae (PN).

Infrared (IR) spectroscopy is used to probe the nature of SiC dust grains in space because dust particles of a given size, shape, temperature, structure, and composition have their own signature IR spectrum. Dust grains absorb high energy photons from stars and re-emit in the IR, in accordance with the specific (low) temperatures of any given grain. Therefore, to account for the energy budget in astronomical environments, astrophysicists are also interested in how SiC dust grains absorb and scatter UV-vis photons, which requires knowledge of SiC optical functions. Lines of evidence or constraints that astrophysicists use to aid studies of SiC dust in space include evidence from meteoritic studies, comparisons between the positions and shapes of spectral features for astronomical objects and laboratory analogue materials, spatial distributions of materials, and theoretical models for dust formation.

## 2. Silicon carbide in meteorites

SiC particles were the first presolar dust grains found in meteorites (Bernatowicz et al., 1987) and remain the best studied (e.g. Clayton & Nittler, 2004; Bernatowicz et al., 2006; Hoppe, 2009). Presolar grains are ancient refractory dust with the isotopic makeup of stars that exist as individual particles or clusters found in the matrix, or fine-grained crystalline mass, of a meteorite. Ages of meteoritic SiC grains are discussed by Ott (2010). Figure 3 describes the family of meteorite classes that contain presolar SiC grains. The most studied meteorites that contain presolar SiC are carbonaceous chondrites (e.g., the class CM2 Murchison and Murray meteorites, classes CI1 = Orgueil, CV3 = Allende) which are considered to be the most primitive or least processed solid materials in the Solar System. Presolar SiC is also found in other stony meteorite types as well: enstatite chondrites (e.g., EH4 = Indarch, EH3 = Qingzhen) and ordinary chondrites (e.g., H/L 3.6 = Tieschitz, LL 3.1 = Bishunpur, Krymka, LL 3.5 = Chainpur, L/LL 3.4 = Inman; LL 3.0 = Semarkona). Investigations via scanning and transmission electron microscopy have revealed the physical morphology of presolar SiC grains (Figure 4). Whereas presolar grains are rare (Clayton & Nittler, 2004) and very small (typically less than 1  $\mu\text{m}$  in size: Amari et al., 1994), presolar SiC grains are more abundant than other presolar compositions (up to 30 ppm in the Murchison meteorite: Ott & Merchel, 2000) and, at 1.5 nm to 26  $\mu\text{m}$  in size, many are large enough to be probed for their isotopic composition (Yin et al., 2006; Speck et al. 2009, and references therein).

As discussed in the introduction, SiC presolar grains are identified by their anomalous isotopic compositions. In fact, their isotopic compositions have not only identified their likely cosmic sources, but also have provided key tests of hypotheses for nucleosynthesis (element creation) and generate the data needed to refine those hypotheses. Whereas ~1% of presolar SiC probably emanates from stellar environments such as novae and supernovae, the vast majority have isotopic compositions consistent with formation around AGB stars. Because the s-process is the dominant method of forming heavy elements in AGB stars, the SiC grains that form within AGB stellar envelopes are excellent tracers of unadulterated s-process isotopes. Studies of these presolar grains are used to determine s-process timescales, stellar temperature and masses, and neutron exposure rates of stellar nuclei.

Compared to solar isotopes, presolar SiC grains exhibit anomalous isotopic compositions for their major components C and Si, as well as trace elements: N, Mg, Ca, Ti, Sr, Zr, Mo, Ba, Nd, Sm, Dy, and the noble gases (Hoppe & Ott, 1997). Based on such isotopic analyses, six types of presolar SiC have been established according to their Si,  $^{12}\text{C}/^{13}\text{C}$ ,  $^{14}\text{N}/^{15}\text{N}$ , and  $^{26}\text{Al}/^{27}\text{Al}$  ratios (e.g., table 2, Ott, 2010 and references therein): “mainstream” SiC, versus

types A, B, X, Y, and Z. The “mainstream” SiC population, constituting ~ 87-94% of known presolar SiC grains, is believed to have originated around C-rich AGB stars. Compared to “mainstream” SiC, A and B SiC grains have low  $^{12}\text{C}/^{13}\text{C}$  but a similar Si profile; they are thought to derive from a particular class of C-star. Y and Z SiC grains are typically small as compared to other presolar SiC grains, are easily distinguished from the “mainstream” class by their Si content, and come from either low mass, low metallicity AGB stars that undergo different types of processing or possibly novae. Type X SiC grains are the most rare (~1% of presolar SiC), are generally collections of many < 100 nm-sized rather than individual grains, and have been proposed to derive from ejecta of core-collapse (Type II) supernovae.

Laboratory studies of presolar meteoritic SiC grains have utilized and developed many innovative techniques (see review by Hoppe, 2009). Initial works relied on ion microprobe and secondary ion mass spectrometry (SIMS) techniques to determine isotopic compositions for light and intermediate mass elements in individual presolar SiC grains, including C, N, Si, Ca, Ti, Mg, Al, O, V, Fe, Sr, Y, Zr, Nb, Ba, Ce, Nd, B (Amari et al., 1992, 1995, 1996, 1997a, 1997b; Hoppe et al. 1994a, 1994b, 1996, 2000, 2001). Post 2001, efforts to drive down the diameter of the primary ion beam and thus be able to probe presolar grains smaller than 0.5  $\mu\text{m}$  resulted in a series of studies using the Cameca NanoSIMS 50 ion microprobe (Besmehn & Hoppe, 2002; Hoppe & Besmehn, 2002; Gyngard, 2009). Time-of-flight secondary ion mass spectrometry (TOF-SIMS) has been applied to submicron presolar SiC grains in an effort to sputter less sample (Henkel et al., 2007), and atomic probe tomography (field ion microscope + TOF mass spectrometer) has also been tested on presolar and synthetic SiC grains to significantly improve upon the spatial resolution of NanoSIMS (Heck et al., 2010). Resonance ion mass spectrometry (RIMS) studies have further quantified the isotopic compositions of heavy elements such as Zr, Mo, and Ba in presolar SiC grains (e.g., Nicolussi et al., 1997, 1998; Savina et al., 2003; Barzyk, 2007). Laser heating experiments by Nichols et al. (1992) and later work by Heck (2005) have yielded the isotopic compositions of He and Ne in presolar SiC. Combinations of SIMS, RIMS, gas mass spectrometry, and other experimental methods (e.g., SEM, TEM, Auger spectroscopy) are currently being employed in analyses of presolar SiC grains (cf. Stroud et al., 2004).

A subset of studies on the isotopic compositions of presolar SiC grains investigates the effect of grain sizes on concentrations of s-process elements. Prombo et al. (1993) found a correlation between grain size and the concentration of s-process elements in the presolar SiC grains taken from the Murchison meteorites. Presolar SiC grains from the Indarch meteorite yielded similar results (Jennings et al., 2002). In both cases, the smaller grains have higher relative abundances of s-process elements.

In addition to the isotopic studies of presolar SiC, crystallographic studies have shown that nearly all are of the  $\beta$ -polytype (cubic crystal structure) and the 6H- $\alpha$ -polytype is never found. In the Murray C2 carbonaceous chondritic meteorite in which presolar SiC was first unequivocally detected, cubic and {111}-twinned cubic were the most common structural forms (Bernatowicz et al. 1987, 1988a, 1988b). Daulton et al. (2002, 2003) itemize the amount of 3C  $\beta$ -SiC (80%), 2H  $\alpha$ -SiC (3%), and intergrowths of these two forms (17%) present in presolar SiC grains. This is significant in astrophysics because which polytype of SiC forms in space strongly depends on the temperature and gas pressure within the dust-forming region. 2H and 3C are the polytypes that form at the lowest temperature where SiC condenses; which of 2H or 3C SiC forms depends on many factors, such as Si/C ratio.

For further reviews of SiC and cosmic dust in meteorites, see also Anders & Zinner (1993), Hoppe & Ott (1997), Hoppe & Zinner (2000), Hoppe (2009), Ott (2010), and Henning (2010).

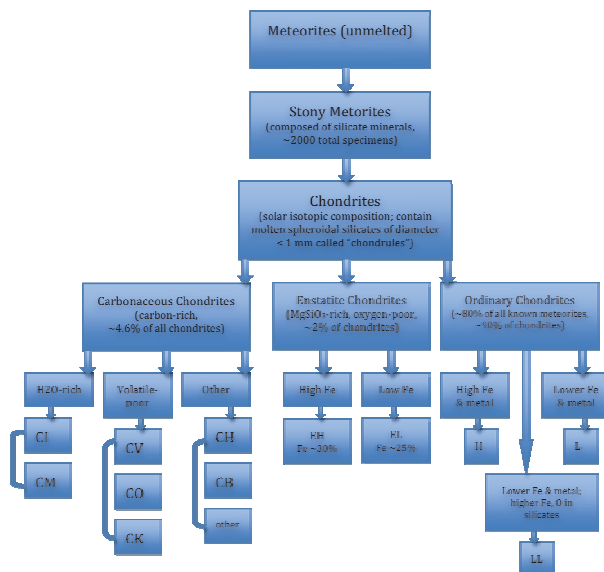


Fig. 3. Meteorite classification formalism, adapted from The Natural History Museum, London (<http://www.nhm.ac.uk>). Presolar SiC grains are dominantly found in the carbonaceous chondrite classes CM, CI, and CV, but occur over a range of subclasses. The numbers (e.g., the "2" in "CM2") represent the petrologic grade of the meteorite (Van Schmus & Wood, 1967); "1" or "2" refers to the degree of hydration or aqueous alteration, whereas for a value of 3 or greater, higher numbers imply successively higher degrees of thermal metamorphism.

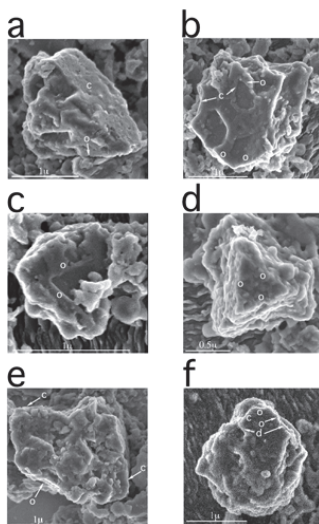


Fig. 4. Microscopy images of pristine presolar SiC grains, courtesy of T. Bernatowicz. Scale bar = 1 µm for all images except panel (d) = 0.5 µm.

### 3. Laboratory astrophysics of silicon carbide

For SiC, the major spectral features result from cation-anion charge transfer and/or electronic band gap transitions in the visible-UV, as well as from lattice vibrations in the IR. Vibrational motions involving a change in the dipole moment are IR active. The nearest-neighbor interaction between Si and C produces a strong band in the IR, regardless of polytype. The stacking disorder that exists for SiC lowers crystal symmetry, resulting in vibrational transitions that increase in number with polytype complexity. For all polytypes of SiC, the transverse optic mode (TO) is present at  $\sim 12.5 \mu\text{m}$  and the longitudinal optic mode (LO) is seen at  $\sim 10.3 \mu\text{m}$  (Nakashima & Harima, 1997). Electronic transitions occur throughout the visible-UV and are strongest at  $\sim 0.111 \mu\text{m}$  (Philipp & Taft, 1960). Laboratory astrophysics studies focus on low energy or IR wavelength SiC spectral features (at  $\lambda \sim 11 \mu\text{m}$ ,  $21 \mu\text{m}$ ) to identify cosmic SiC in space, and also quantify the optical depth of and chemical impurities or defects in cosmic SiC via the general spectral behavior of the UV.

#### 3.1 Spectroscopic studies: Ultraviolet and infrared

Past laboratory spectral studies utilized by astrophysicists are published across multiple disciplines. Although UV measurements for other sample types, e.g., extinction of light from SiC smoke particles (Stephens, 1980), have also been used in astrophysics, this paragraph reviews the state of single-crystal SiC spectroscopic studies in the UV and gives examples of UV SiC spectra in Figures 5 and 6. The polytypes that matter most to astrophysicists are 3C, 2H, and 4H, on the basis of the meteoritic record; data on other forms (e.g., 8H, 15R, 21R) have not been considered. Because the 6H form of  $\alpha$ -SiC is available commercially with large faces perpendicular to  $c$  axis, for which unpolarized measurements provide data on  $E \perp c$ , there is a wealth of laboratory spectra on 6H in this orientation. The first  $\alpha$ -SiC laboratory reflectance data (e.g., Philipp, 1958; Wheeler, 1966) were gathered at resolutions lower by at least a factor of two than can be attained with modern instrumentation. In the ultraviolet, modern commercial instruments exist and are inexpensive for wavelengths down to  $0.192 \mu\text{m}$  (or, for a factor of  $\times 10$  more in cost, down to  $0.164 \mu\text{m}$ , the "vacuum UV"). However, spectral data for SiC used by astrophysicists does not extend much past  $200 \text{ nm}$ , as summarized in Figure 5. Early works on UV SiC spectroscopy studied in the astrophysics literature include Choyke & Patrick (1957), Philipp (1958), and Philipp & Taft (1960). Choyke & Patrick (1957) measured transmission (converted to absorption coefficient in  $\text{cm}^{-1}$ ) for one  $\alpha$ -SiC plate, whereas Philipp (1958) measured absorption for yellow 3C and colorless 6H SiC single crystal samples of varying thicknesses. In both studies, samples were not well characterized in terms of SiC impurities, stacking faults, and defects, which are highly important in the UV-vis. Philipp & Taft (1960) presented reflectance spectra from  $\sim 0.11$  to  $0.62 \mu\text{m}$  for hexagonal SiC. Because reliable reflectivity standards were not available at that time, uncertainties in absolute  $R$  were large (i.e.,  $> 5\%$ ). Hofmeister et al. (2009) published new data on the visible to soft UV range ( $1.11$ - $0.303 \mu\text{m}$ ) for  $\alpha$ - and  $\beta$ -SiC single crystals with emphasis on impurities. In that study, absorbance spectra were provided for 6H and 3C SiC ( $E \parallel c$  and  $E \perp c$ ) as electronic tables for  $\lambda = 2.5$ - $16.36 \mu\text{m}$ ; figure 7 of that work provides absorbance spectra shortward of  $2.5 \mu\text{m}$ . Additional laboratory UV absorption spectra (e.g., Choyke & Patrick 1968, 1969) and reflectivity spectra, including experimentally measured and calculated data (Wheeler, 1966; Belle et al., 1967; Lubinsky et al., 1975; Rehn et al., 1976; Gavrilenko, 1995; Logothetidis & Petalas, 1996; Adolph et al., 1997; Gavrilenko & Bechstedt,

1997; Theodorou et al., 1999; Ismail & Abu-Safia, 2002; Xie et al., 2003; Lindquist et al., 2004) that extend into the vacuum UV are available in the semiconductor literature. In particular, the effect of SiC polytype on reflectivity was discussed by Lambrecht et al. (1993, 1994, 1997); we note that the reflectivity values from Lambrecht et al. (1997) are too low by 20%, caused by calibrating against a low value of real index of refraction ( $n=2.65$ ) at  $\sim 0.31 \mu\text{m}$  (e.g., Petalas et al., 1998). The spectroscopic ellipsometry study by Petalas et al. (1998) provides reflectivity in agreement with Philipp & Taft (1960) and Wheeler (1966). The reflectivity data by Wheeler (1966) have been used extensively in comparison in the physics and materials literature but show structure on the spectral peaks that may not be real since those features were not observed subsequently; thus, those data are not shown explicitly in Figure 5. For further discussion, see the review by Devaty & Choyke (1997).

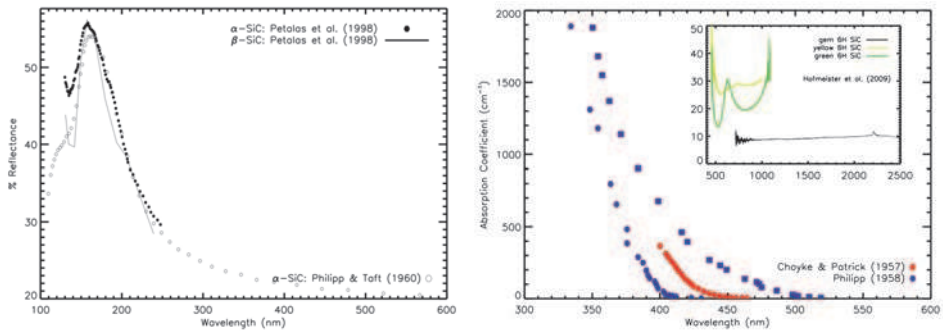


Fig. 5. UV-visible reflectance spectra and absorption coefficients.  $1 \text{ nm} = 10^{-3} \mu\text{m}$ . Panel (a): Open symbols: Philipp & Taft (1960), solid symbols and line: Petalias et al. (1998). Panel (b): Squares = 3C SiC, hexagons = 6H SiC. Inset: gem 6H SiC = synthetic moissanite.

In the infrared, many laboratory studies of SiC are available in astrophysics, some of which should be compared to semiconductor-relevant data with care. Spitzer et al. (1959a) obtained reflectivity data from a thin ( $0.06 \mu\text{m}$ ) film of  $\beta$ -SiC that was vapor-deposited on a Si surface. Spitzer et al. (1959b) provided laboratory data for both polarizations of 6H single-crystals. Another widely cited source in astrophysics is the  $\alpha$ -SiC E<sub>Lc</sub> data shown in figure 9.6 of Bohren & Huffman (1983); that work did not provide experimental details, such as which polytype of  $\alpha$ -SiC was used. Mutschke et al. (1999) presented averages of spectral parameters from many experimental studies of SiC from the 1960's to 1990's to obtain TO frequency positions, LO frequency positions or oscillator strengths, and full width at half maximum values for SiC. Other published works on SiC from astrophysics (e.g., Friedemann et al., 1981; Borghesi et al., 1985; Orofino et al., 1991; Papoular et al., 1998; Mutschke et al., 1999; Andersen et al., 1999, and references therein) are predominantly laboratory absorbance studies of powder samples, embedded in a (usually KBr) matrix. Strong differences in the spectra and optical properties obtained from powders (cf. Huffman, 1988; Mutschke et al., 1999) can be attributed to variations in clustering of grains, dilution, mean and distributions of grain size and shape. Laser pyrolysis has also been used to produce SiC particles most closely resembling those found in stellar environments (cf. Willacy & Cherchneff, 1998; Mutschke et al., 1999). Because the laser pyrolysis SiC samples are not of the order of several mm in diameter (cf. Hofmeister et al., 2003), those

measurements should not be used for determining bulk optical functions. A wavelength shift (the KBr matrix correction, cf. Friedemann et al., 1981) has been applied to some laboratory spectra of sub- $\mu\text{m}$  SiC grains dispersed in single-crystal matrices. Studies of thin films and isolated nanoparticles of  $\beta\text{-SiC}$  have shown that this wavelength shift is unnecessary when measurements are made carefully (Speck et al., 1999; Clément et al., 2003). Past astrophysical studies were also divided on whether the crystal structure of SiC can be determined from IR spectra (in favor: Borghesi et al., 1985; Speck et al., 1999; opposed: Spitzer et al., 1959a, 1959b; Papoular et al., 1998; Andersen et al., 1999; Mutschke et al., 1999). Pitman et al. (2008) showed that spectroscopic differences exist between  $\alpha\text{-SiC}$  ( $E \parallel c$ ), versus  $\beta\text{-SiC}$  or  $\alpha\text{-SiC}$  ( $E \perp c$ ). Pitman et al. (2008) provided electronic mid- and far-IR room temperature reflectance spectra of thin film 6H SiC (two orientations, several varieties) and semiconductor grade purity 3C SiC.

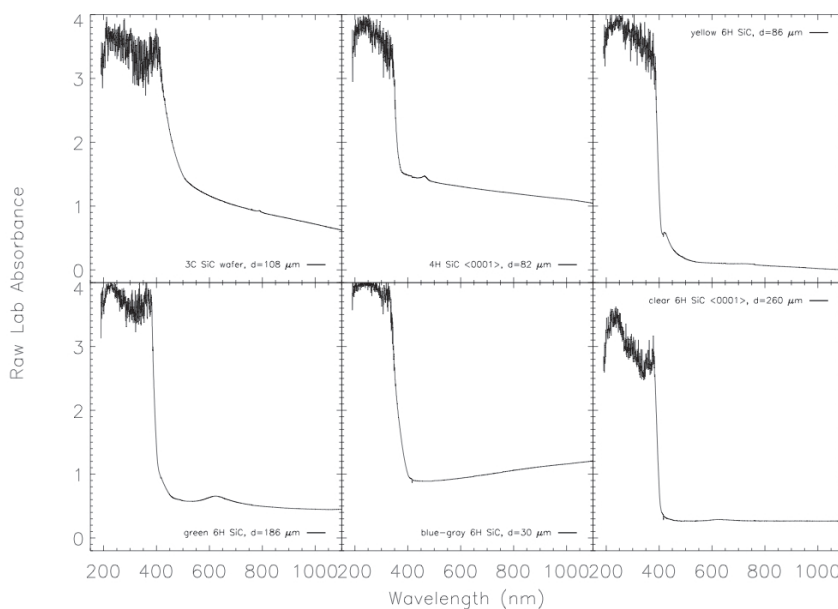


Fig. 6. Comparing the effects of color impurities and polytype of SiC in the UV-vis.  $1 \text{ nm} = 10^{-3} \mu\text{m}$ .  $d$  = thickness of sample. Vertical axis given in common log absorbance.

The two SiC spectral features of greatest interest to astrophysicists are at 11 and 21  $\mu\text{m}$ . The utility of the 11  $\mu\text{m}$  feature (shown in Figure 7) will be discussed in Section 4. Among the C-rich post-AGB stars (PPNe), approximately half exhibit a feature in their infrared spectra at 21  $\mu\text{m}$ . This enigmatic feature has been widely discussed since its discovery (Kwok et al., 1989) and has been attributed to both transient molecular and long-lived solid-state species, but most of these species have been discarded. The most promising carrier is SiC (Speck & Hofmeister, 2004), on the basis of lab spectroscopy (Figure 8). The peak positions and profile shapes of the 21  $\mu\text{m}$  band are remarkably constant, both in space (Volk et al., 1999) and in laboratory SiC spectra (Table 1). Kimura et al. (2005a, 2005b) produced nano-diamond

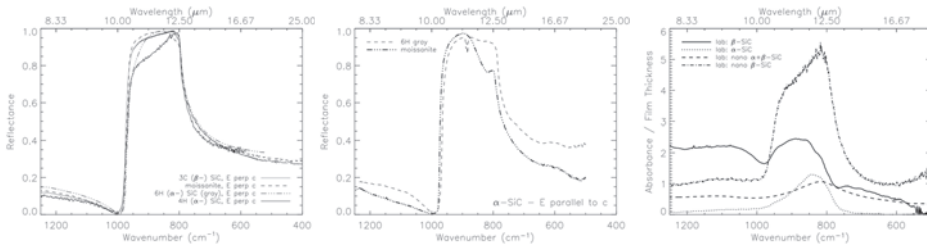


Fig. 7.  $\lambda \sim 11 \mu\text{m}$  feature in SiC. Panels (a, b): Mid- and mid+far-IR specular reflectivity spectra of bulk SiC, for different orientations. Panel (c): Laboratory (common log) absorbance, divided by thin film thickness for bulk versus nanocrystalline  $\beta$ -SiC,  $\alpha$ -SiC, and a mixture of the two. Data from this work, K. M. Pitman et al., A&A, vol. 483, pp. 661-672, 2008, reproduced with permission © ESO.

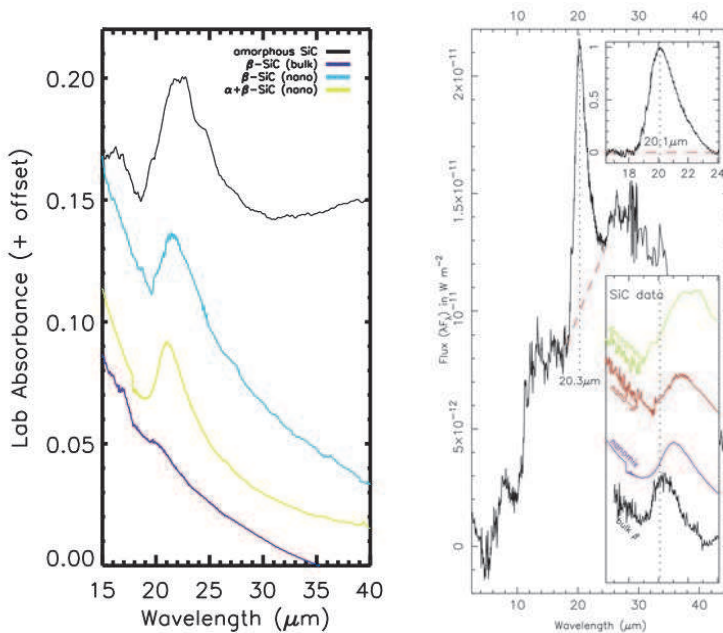


Fig. 8. The  $\lambda \sim 21 \mu\text{m}$  feature in the SiC laboratory spectra is prominent in nanocrystalline and amorphous SiC, present but not as strong in bulk SiC. Laboratory IR absorbance spectra of SiC shown in bulk, nanocrystalline, amorphous, blends of  $\alpha$ - and  $\beta$ -SiC. Some data from Speck & Hofmeister (2004); new  $\beta$ -SiC nanocrystalline data included longward of  $20 \mu\text{m}$ . At  $19.8 \mu\text{m}$ , a “S-shaped” beamsplitter artifact or spectral spike occurs. The amorphous SiC sample was polycard (i.e., this spectrum has a different baseline than the other 3 spectra, most noticeable at  $\lambda > 21 \mu\text{m}$ ). The amorphous SiC spectrum was offset by -0.19 in vertical axis; the other spectra were not offset. Instrumental noise was smoothed for amorphous SiC at  $\lambda < 20 \mu\text{m}$  and again for nanocrystalline  $\beta$ -SiC spectra at  $\lambda > 27 \mu\text{m}$ . The steep rise to short  $\lambda$  occurs because this feature is a shoulder on the main band near  $11 \mu\text{m}$ .

	Position (cm <sup>-1</sup> )	Height	Width
Amorphous SiC	450.172	0.1340	102.16
Nanocrystalline $\beta$ -SiC	463.52	0.09291	34.3971
	424.75	0.07975	58.4357
Nanocrystalline $\alpha$ + $\beta$ SiC	472.69	0.1274	60.794
	433.09	0.03869	74.790

Table 1. Peak parameters of  $\lambda \sim 21 \mu\text{m}$  feature in SiC. Values reported in frequency (cm<sup>-1</sup> = 10<sup>4</sup>/ $\lambda(\mu\text{m})$ ). Amorphous SiC spectrum was best fitted with a single Gaussian peak and multi-point baseline correction. Peaks in the IR actually tend to be Lorentzian in shape; the 21  $\mu\text{m}$  feature in the nanocrystalline spectra were fitted with two Lorentzian peaks (for the TO and LO modes) and a two-point linear baseline correction.

samples with Si replacing C from 10 to 50% by various methods; its IR spectrum exhibits bands at 9.5 and 21  $\mu\text{m}$ , and the relative strength of the 21  $\mu\text{m}$  band increases with C content. On this basis, Kimura et al. (2005a, 2005b) concluded that the 21  $\mu\text{m}$  band in IR spectra of SiC samples also results from excess C. Jiang et al. (2005) calculated IR spectra of astronomical dust for various sub- $\mu\text{m}$  grain sizes and a range of peak strengths for the 21  $\mu\text{m}$  band at  $T \sim 70 \text{ K}$ . That work concluded that the 21  $\mu\text{m}$  feature was too weak to be SiC unless very high concentrations of impurity were observed. However, relative peak intensities are affected by factors not explored in that study. The intensity of emission at 21  $\mu\text{m}$  would be enhanced relative to that at 11  $\mu\text{m}$  by either lower temperature or larger (non-uniform) grain sizes. A more serious objection to the assignment is that the astronomy environment could possess Si-rich nano-diamond. Quantifying the strengths of the 21  $\mu\text{m}$  SiC feature in both structures and low temperature measurements is needed to differentiate between these possibilities.

### 3.2 Optical functions of SiC

Optical functions or “optical constants” are the real and imaginary parts of the complex index of refraction  $m = n + ik$  that vary as a function of wavelength, temperature, and dust species (composition, structure).  $n(\lambda)$  is the real index of refraction where the crystal is not strongly absorbing, and  $k(\lambda) = A/4\pi v$  represents the extinction or gradual loss of intensity due to absorption of photons as an electromagnetic wave interacts with matter. As discussed in the introduction, there is a substantial market for the optical functions of SiC within the astrophysics community. In the IR, the optical functions of SiC used in 20th century astronomical studies derive primarily from three studies: Bohren & Huffman (1983), Pégourié (1988), and Laor & Draine (1993). These data were for  $\alpha$ -SiC, often in a single polarization, whereas SiC dust surrounding astronomical objects is  $\beta$ -SiC, and included a wavelength shift to “correct” for the KBr matrix. Pitman et al. (2008) derived and provided electronic tables of SiC optical functions out to  $\lambda \sim 2000 \mu\text{m}$  for 6H ( $\alpha$ -)SiC in both polarizations as well as 3C ( $\beta$ -)SiC; Hofmeister et al. (2009) extended these data shortward into the UV. For all spectral regions, the latter papers showed that 3C SiC and the  $E \perp c$  polarization of 6H SiC have almost identical optical functions that can be substituted for each other in modeling astronomical environments. This result agreed with previous work

by Mutschke et al. (1999). However, optical functions for the E || c orientation of 6H SiC can differ slightly (peaks shifted to lower frequency). Figure 9 presents optical functions for 4H SiC, with comparison to the other polytypes from Pitman et al. (2008), and optical functions comparing colored versus colorless samples of SiC from Hofmeister et al. (2009). In the UV,  $n$  and  $k$  were also calculated for 6H SiC at  $\sim 0.25\text{--}1.24\ \mu\text{m}$  by Obarich (1971) and Ninomiya & Adachi (1994); works presented above also included calculated dielectric functions for other polytypes, from which one may further obtain  $n$  and  $k$  in the UV.

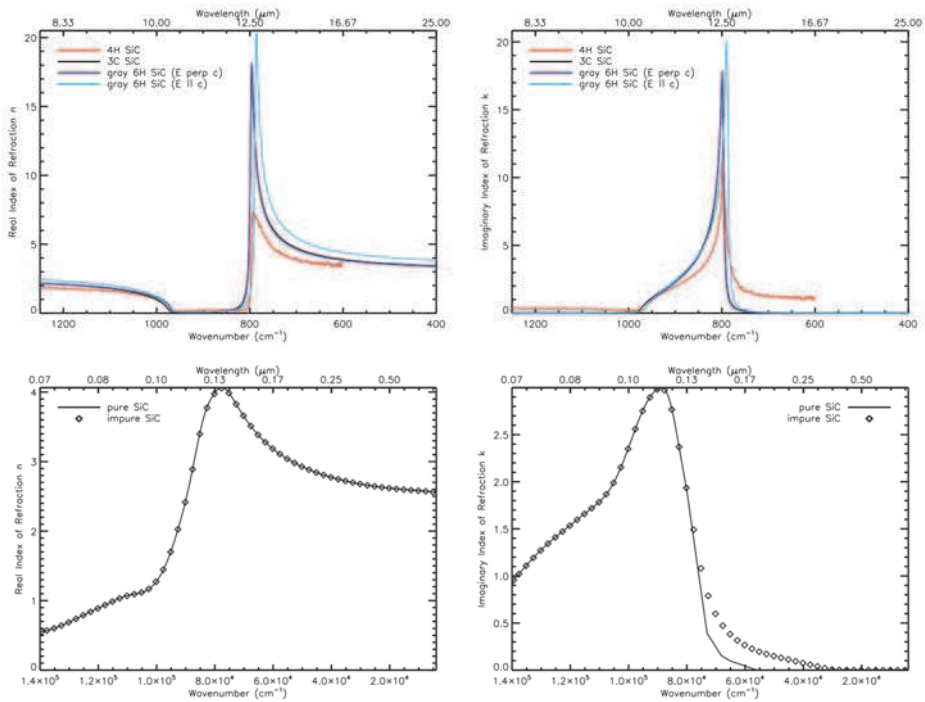


Fig. 9. UV-vis optical functions derived from experimental specular reflectance data via Lorentz-Lorenz classical dispersion analysis, showing the effect of polytype (top panels; 3C and 6H from Pitman et al. 2008, 4H from this work) and of impurities (bottom panels; Hofmeister et al. 2009, applicable to 3C or 6H E  $\perp$  c). Left: real index of refraction  $n$ . Right: imaginary index of refraction  $k$ . With the exception of 6H SiC E || c orientation, the optical functions for SiC are generally similar, regardless of polytype. As compared to 99.8% pure (colorless) SiC samples, the effect of impurities in colored SiC samples manifests in  $k$ .

#### 4. Application #1: Observational astronomy

In this section, we outline the ways in which astrophysicists compare laboratory spectra and optical functions of SiC to determine the nature and evolution of SiC dust grains around classes of astronomical objects and environments, e.g., C-rich AGB stars (i.e., carbon stars).

#### 4.1 Matching spectral features

The first step in identifying the nature of dust grains in space is to match the positions and widths of astronomically observed spectral features with those seen in laboratory spectra. To do this we must consider what actually contributes to the spectrum when we look at a dusty star. The spectrum,  $F_\lambda$ , is made of contributions to the light from the star (which is essentially a blackbody, or perfect light absorber at all wavelengths) and the circumstellar material. In the infrared, the circumstellar material is dominated by the dust, the emission from which is determined by the species, i.e., composition, crystal structure, size, and shape of the grains. The spectrum can be represented by Eq. 1,

$$F_\lambda = \sum_{i=1, j=1}^{n, m} w_j \times Q_j \times B_i \quad (1)$$

where  $B_\lambda(T)$  is the Planck function for a black body of temperature  $T$ , so that  $B_i$  represents a single dust grain at a single temperature (of which there are  $n$  in total). Each  $Q_j$  represents the extinction efficiency (or rate at which a dust particle absorbs, scatters, or extinguishes light divided by the incident power per unit area) for a single grain type as defined by its size, shape, composition and crystal structure. Each  $w_j$  represents the weighting factor for a single grain type (of which there are  $j$  in total).

For optically thin environments, where there is little or only single-scattering, the spectrum is dominated by starlight, and one can simply subtract a blackbody continuum relevant to the star (which for carbon stars is  $\sim 3000$  K). However, for very dusty environments, starlight is largely absorbed by the dust and re-emitted in the infrared according to the dust grains' optical functions. Often the system is simplified so that the contributions to the spectrum are dominated by a single dust species and Eq. 1 simplifies to Eq. 2,

$$F_\lambda = w \times Q_\lambda \times B_\lambda(T) \quad (2)$$

In this case one can fit a (blackbody) continuum to the observed spectrum and divide to derive emissivities of the observed spectral features (e.g., Speck et al. 1997).

The circumstellar shells of carbon stars are expected to be dominated by amorphous or graphitic carbon grains (see Speck et al. 2009 and references therein). These dust species do not have diagnostic infrared features, and contribute to the dust continuum emission alone. However, SiC does exhibit a strong infrared feature around  $11\mu\text{m}$  as discussed in Section I. The observed  $\sim 11\mu\text{m}$  SiC feature has been used extensively to investigate the nature and evolution of dust around carbon stars (Little-Marenin, 1986; Baron et al., 1987; Willems, 1988; Chan & Kwok, 1990; Goebel et al., 1995; Speck et al., 1997; Sloan et al., 1998; Speck et al., 2005; Thompson et al., 2006; Speck et al., 2009), using datasets from both space-based instruments such as the Infrared Astronomical Satellite (IRAS) Low Resolution Spectrometer (LRS: Neugebauer et al., 1984), and the Infrared Space Observatory (ISO: Kessler et al., 1996) Short Wavelength Spectrometer (SWS: de Graauw et al., 1996), as well as instruments in ground-based observatories (e.g., CGS3 on the United Kingdom Infrared Telescope, UKIRT). In fact, the parameters most commonly used to make identifications of SiC dust in space are the strength and peak position of the  $\sim 11\mu\text{m}$  feature. From ISO data, there is also a range in shapes and peak positions of the  $\sim 11\mu\text{m}$  SiC feature that cannot be simply correlated with the apparent temperature of the

underlying continuum (Thompson et al., 2006). However, there remain several common trends that exist in the observed SiC features:

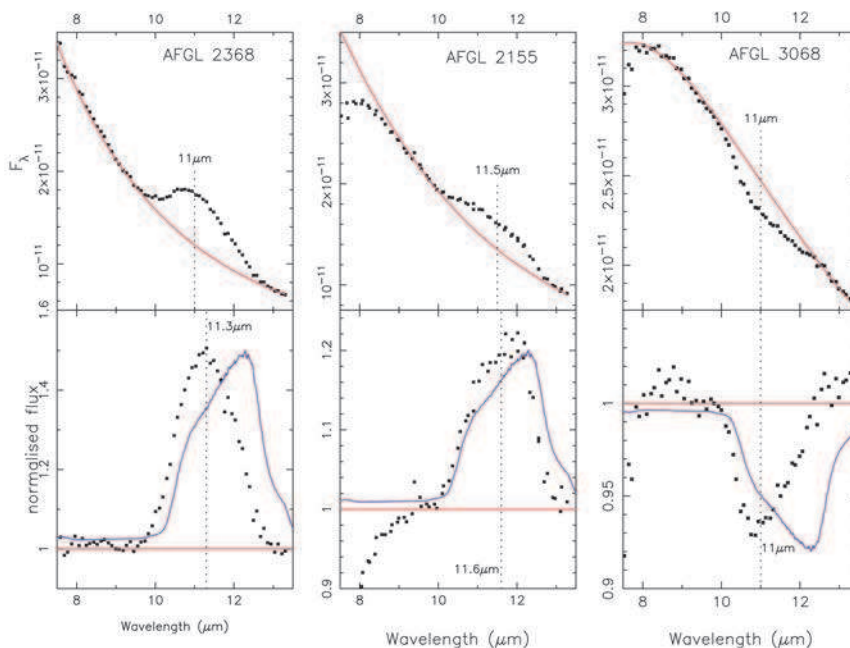


Fig. 10. The 11  $\mu\text{m}$  SiC feature, observed in the spectra of carbon stars. Left hand panels represent stars that have the optically thinnest dust shells; optical depth increases to the right. Top panels: Ground-based observed spectra (black symbols: Speck et al. 1997) with best-fitting blackbody continua (red lines). Bottom panels: Continuum-divided spectra, following Eq. 2, provide the effective Q-values or extinction efficiencies for the dust shells. Blue lines:  $\beta$ -SiC absorbance data of Pitman et al. (2008), converted to absorptivity  $A = e^{\text{absorbance}}$ , is proportional to Q.

- i. Early in the AGB phase, when the mass-loss rate is low and the shell is optically thin, the  $\sim 11 \mu\text{m}$  SiC emission feature is strong, narrow, and sharp.
- ii. As the mass loss increases and the shell becomes optically thicker, the SiC emission feature broadens, flattens, and weakens.
- iii. Once the mass-loss rate is extremely high and the shell is optically thick, the SiC feature appears in absorption.
- iv. Once the AGB phase ends and the thinning dust shell cools, SiC is more rarely observed but may be hidden by other emerging spectral features.

## 5. Application #2: Radiative transfer modeling

Radiative transfer (RT) modeling uses the optical functions of candidate minerals to model how a given object should look both spectroscopically and in images. Mineral candidates determined by spectral matching can then be input into numerical RT models; examples of

codes used to solve the equation of radiative transfer are DUSTY (Nenkova et al. 2000) and 2-Dust (Ueta & Meixner 2003). The acquisition of new optical functions, for SiC and all materials posited to exist in space, is critical to these numerical efforts. Astrophysicists use RT modeling to determine the effects of grain size and shape distributions, chemical composition and mineralogies, temperature and density distributions on the expected astronomical spectrum, and to place constraints on the relative abundances of different grain types in a dust shell. In this way, astrophysicists can build a list of parameters that describes the circumstellar environment around a star.

In radiative transfer modeling, one simulates SiC dust in space by specifying best estimates for the optical functions, sizes, and shape distributions of the particles. The optical functions mentioned in Section 3 have been tested in a variety of radiative transfer applications. The optical functions of Bohren & Huffman (1983), Pégourié (1988), and Laor & Draine (1993) were used to place limits on the abundance of SiC dust in carbon stars (e.g., Martin & Rogers 1987; Lorenz-Martins & Lefevre 1993, 1994; Lorenz-Martins et al. 2001; Groenewegen 1995; Groenewegen et al. 1998, 2009; Griffin 1990, 1993; Bagnulo et al. 1995, 1997, 1998), Large Magellanic Cloud stars (Speck et al. 2006; Srinivasan et al. 2010), and (proto-)planetary nebulae (Clube & Gledhill 2004; Hoare 1990; Jiang et al. 2005). Those optical functions have also been used in studies of dust formation (e.g., Kozasa et al. 1996), hydrodynamics of circumstellar shells (e.g., Windsteig et al. 1997; Steffen et al. 1997), and mean opacities (Ferguson et al. 2005; Alexander & Ferguson 1994). In their radiative transfer models of dust around C-stars, Groenewegen et al. (2009) offered a comparison of the performance of the optical functions of Pitman et al. (2008), shown in Figure 3.5, against  $\alpha$ -SiC from Pégourié (1988), and  $\beta$ -SiC from Borghesi et al. (1985) in matching observed 11  $\mu\text{m}$  features in astronomical spectra. Ladjal et al. (2010) concluded that the Pitman et al. (2008) modeled the shape and peak position of the 11  $\mu\text{m}$  feature well in evolved stars. The intrinsic shape for SiC grains in circumstellar environments is not known but distributions of complex, nonspherical shapes (Continuous Distribution of Ellipsoids, CDE, Bohren & Huffman 1983; Distribution of Hollow Spheres, Min et al. 2003; aggregates, Andersen et al. 2006, and references therein) are the best estimate at present. Most of these produce a feature at  $\lambda \sim 11 \mu\text{m}$  that is broad as compared to laboratory SiC spectra, but matches astronomically observed spectra. There is no clear consensus on what the grain size distribution for SiC grains in space should be (see review by Speck et al. 2009). SiC dust is generally found in circumstellar, not interstellar, dust, which limits the assumptions on size. Strictly speaking, the SiC optical functions of Pégourié (1988) and Laor & Draine (1993) should be used with the corresponding grain size distribution of the ground and sedimented SiC sample measured in the lab ( $\propto \text{diameter}^{-2.1}$ , with an average grain diameter = 0.04  $\mu\text{m}$ ). Bulk  $n$  and  $k$  datasets (e.g., Pitman et al. 2008; Hofmeister et al. 2009) can be used with any grain size distribution.

Once optical functions, sizes, and shape distributions have been selected for the SiC particles, astrophysicists are free to test the influence of percent SiC dust content on an astronomical spectrum. Figure 11 gives examples of synthetic spectra of SiC-bearing dust shells of varying optical thicknesses around a  $T=3000 \text{ K}$  star using the radiative transfer code DUSTY. Simply changing the optical functions and/or shape distribution results in substantial differences in the modeled astronomical spectrum, and thus interpretations of the self-absorption and emission in the circumstellar dust shell.

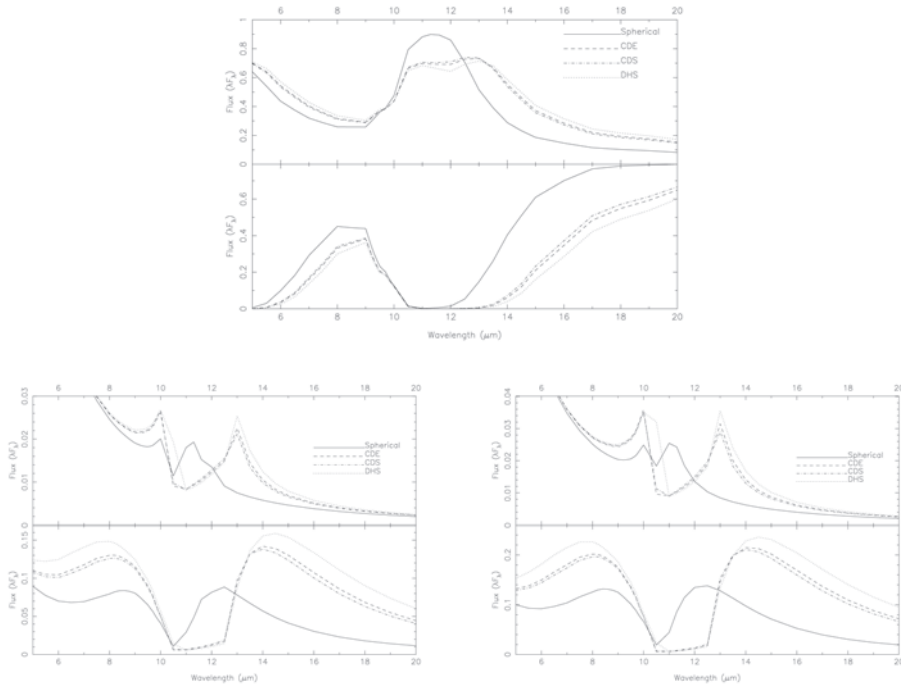


Fig. 12. Synthetic spectra of stellar light flux generated with DUSTY code. Top panel: Pégourié (1988)  $\alpha$ -SiC optical functions. Bottom panel: Pitman et al. (2008) SiC optical functions. Left hand versus right hand columns compare  $\alpha$ -SiC (weighted average of  $1/3 E \parallel c, 2/3 E \perp c$ ) versus  $\beta$ -SiC. Line styles compare different shape distributions (spherical, CDE, CDS = continuous distribution of ellipsoids; spheroids, DHS = distribution of hollow spheres). See Corman (2010) and Corman et al. (2011) for more examples.

## 6. Conclusion

Since the 1960s, laboratory and theoretical astrophysics investigations of SiC grains have culminated in several important findings:

1.  $\sim 99\%$  of meteoritic SiC grains were formed around carbon-rich Asymptotic Giant Branch stars, and that of these,  $> 95\%$  originate around low-mass ( $< 3M_{\odot}$ ) carbon stars;
2. Nearly all SiC grains in space are crystalline, with  $> 80\%$  of these occurring as the cubic 3C polytype, and the rest comprising the lower temperature 2H polytype or 3C/2H combinations;
3. The grain size distribution of SiC in space includes both very small and very large grains (1.5 nm - 26  $\mu\text{m}$ ), with most grains in the 0.1-1  $\mu\text{m}$  range. Single-crystal SiC grains can exceed 20  $\mu\text{m}$  in size. The sizes of individual SiC crystals are correlated with s-process element concentration.
4. There is no consensus on the shape of SiC particles in space. SEM and TEM imagery of presolar SiC grains provides a guide. In numerical radiative transfer model calculations,

distributions of complex, nonspherical shapes (continuous distributions of ellipsoids or hollow spheres; fractal aggregates) are assumed.

5. Complimentary spectroscopic measurements of synthetic SiC made by the semiconductor and astrophysics communities have provided consistent values for optical functions, once different methodologies have been accounted for. Laboratory astrophysics studies of SiC focus on general UV spectral behavior and two specific IR spectral features (at  $\lambda \sim 11 \mu\text{m}$ ,  $21 \mu\text{m}$ ) that can be matched to astronomical spectra. The effects of orientation, polytype, and impurities in SiC are all important to astronomical studies.
6. Variations in optical functions with impurities and structure, as well as assumptions on size and shape distributions, strongly affects the amount of light scattering and absorption inferred in space.

Optical properties of SiC warrant future study. Vacuum UV data from the semiconductor literature need to be better integrated into the astrophysics literature. Laboratory studies on SiC have considered the effect of varying temperature from early on (e.g., Choyke & Patrick 1957). However, most data were collected only at room temperature. Temperature-dependent spectra and optical functions are necessary, especially low-temperature measurements. Chemical vapor-deposited SiC samples are available from the semiconductor industry for  $\beta$ -SiC. For future work, other forms of  $\beta$ -SiC would be better for determining optical functions, e.g., single crystals for the non-absorbing near-IR to visible region. Further measurements of solid solutions of SiC and C, with focus on impurities likely to be incorporated in astrophysical environments rather than doped crystals, should be pursued in the UV. Although IR spectra of 2H SiC can be constructed from available data (e.g., Lambrecht et al. 1997) because folded modes are not present, 2H SiC also warrants direct measurement for its importance in space.

## 7. Acknowledgment

Authors' laboratory and theoretical work shown in this chapter was kindly supported by the National Science Foundation under grants NSF-AST-1009544, NASA APRA04-000-0041, NSF-AST-0607341, and NSF-AST-0607418. Credit: K. M. Pitman et al., *A&A*, vol. 483, pp. 661-672, 2008, reproduced with permission © ESO. Data from Speck & Hofmeister (2004) and Hofmeister et al. (2009) reproduced with permission from the AAS. Figure 2.2 was kindly provided by T. Bernatowicz. The authors thank Jonas Goldsand for his assistance on laboratory sample preparation and data collection. This is PSI Contribution No. 506.

## 8. References

- Adolph, B., Tenelsen, K., Gavrilenko, V. I., & Bechstedt, F. (1997). Optical and loss spectra of SiC polytypes from ab initio calculations, *Phys. Rev. B*, Vol. 55, pp. 1422-1429
- Alexander, D. R., & Ferguson, J. W. (1994). Low-temperature Rosseland opacities, *Astrophys. J.*, Vol. 437, No. 2, pp. 879-891
- Amari, S., Lewis, R. S., & Anders, E. (1994). Interstellar grains in meteorites. I - Isolation of SiC, graphite, and diamond, size distributions of SiC and graphite. II - SiC and its noble gases, *Geochim. Cosmochim. Ac.*, Vol. 58, p. 459.
- Amari, S., Hoppe, P., Zinner, E., & Lewis, R. S. (1992). Interstellar SiC with unusual isotopic compositions - Grains from a supernova?, *Astrophys. J. Lett.*, Vol. 394, pp. L43-L46.

- Amari, S., Hoppe, P., Zinner, E., & Lewis, R. S. (1995). Trace-element concentrations in single circumstellar silicon carbide grains from the Murchison meteorite, *Meteoritics*, Vol. 30, No. 6, p. 679
- Amari, S., Zinner, E., & Lewis, R. S. (1996) CA and TI Isotopic Compositions of Size-Separated SiC Fractions from the Murchison Meteorite, *Lunar Planet. Sci.*, Vol. 27, page 23
- Amari, S., Nittler, L. R., Zinner, E., & Lewis, R. S. (1997a). Presolar SiC Grains of Type A+B, *Meteorit. Planet. Sci.*, Vol. 32, p. A6
- Amari, S., Nittler, L. R., Zinner, E., & Lewis, R. S. (1997b). Continued search for rare types of presolar SiC - Grains X and Y, *Lunar Planet. Sci.*, Vol. 28, p. 33.
- Anders, E., & Zinner, E. (1993). Invited Review - Interstellar grains in primitive meteorites: Diamond, silicon carbide, and graphite, *Meteoritics*, Vol. 28, pp. 490-514
- Andersen, A. C., Loidl, R., & Höfner, S. (1999). Optical properties of carbon grains: Influence on dynamical models of AGB stars, *Astron. Astrophys.*, Vol. 349, pp. 243-252
- Andersen, A. C., Mutschke, H., Posch, Th., Min, M., & Tamanai, A. (2006). Infrared extinction by homogeneous particle aggregates of SiC, FeO and SiO<sub>2</sub>: Comparison of different theoretical approaches, *J. Quant. Spectrosc. Rad. Trans.*, Vol. 100, No. 1-3, pp. 4-15
- Bagnulo, S., Doyle, J. G., & Griffin, I. P. (1995). A study of the size and composition of dust grains in the circumstellar envelope of IRC +10 216, *Astron. Astrophys.*, Vol. 301, p. 501
- Bagnulo, S., Doyle, J. G., & Andretta, V. (1998). Observations and modelling of spectral energy distributions of carbon stars with optically thin envelopes, *Mon. Not. R. Astron. Soc.*, Vol. 296, pp. 545-563
- Bagnulo, S., Skinner, C. J., Doyle, J. G., & Camphens, M. (1997). Carbon stars with detached dust shells: the circumstellar envelope of UU Aurigae, *Astron. Astrophys.*, Vol. 321, pp. 605-617
- Baron, Y., Papoular, R., Jourdain de Muizon, M., & Pégourié, B. (1987). An analysis of the emission features of the IRAS low-resolution spectra of carbon stars, *Astron. Astrophys.*, Vol. 186, p. 271
- Barzyk, J. G. (2007). Multielement isotopic analysis of presolar silicon carbide, Ph.D. thesis (Proquest, AAT 3252254), The University of Chicago, Illinois, USA, 102 pages
- Belle, M. L., Prokofeva, N. K., & Reifman, M. B. (1967). *Soviet Phys. - Semicond.*, Vol. 1, p. 315
- Bernatowicz, T. J., Croat, T. K., & Daulton, T. L. (2006). Origin and Evolution of Carbonaceous Presolar Grains in Stellar Environments, In: *Meteorites and the Early Solar System II*, eds. D. S. Lauretta & H. Y. McSween, Jr. (Tucson: University of Arizona Press), 109
- Bernatowicz, T., Fraundorf, G., Ming, T., Anders, E., Wopenka, B., Zinner, E., & Fraundorf, P. (1987). Evidence for interstellar SiC in the Murray carbonaceous meteorite, *Nature*, Vol. 330, No. 24, p. 728-730
- Bernatowicz, T., Fraundorf, G., Fraundorf, P., & Tang, M. (1988a). TEM Observations of Interstellar Silicon Carbide from the Murray and Murchison Carbonaceous Meteorites, *51st Meeting of the Meteoritical Society*, July 18-22, 1988, Fayetteville, Arkansas, No. 665, p.1

- Bernatowicz, T., Fraundorf, G., Fraundorf, P., & Ming, T. (1988b). TEM Observations of Interstellar Silicon Carbide from the Murray and Murchison Carbonaceous Meteorites, *Meteoritics*, Vol. 23, p. 257
- Bernatowicz, T. J., Akande, O. W., Croat, T. K., & Cowsik, R. (2005). Constraints on Grain Formation around Carbon Stars from Laboratory Studies of Presolar Graphite, *Astrophys. J.*, Vol. 631, p. 988
- Besmehn, A., & Hoppe, P. (2002). NanoSIMS Study of an Unusual Silicon Carbide X Grain from the Murchison Meteorite, *Meteorit. Planet. Sci.*, Vol. 37, Supplement, p. A17
- Blöcker, T., & Schönberner, D. (1991). New pre-white dwarf evolutionary tracks, In: *White Dwarfs*, NATO Advanced Science Institutes (ASI) Series C, Vol. 336, eds. G. Vauclair, E. Sion, p. 1, Kluwer, Dordrecht
- Bohren, C. F., & Huffman, D. R. (1983). *Absorption and Scattering of Light by Small Particles*, John Wiley & Sons Inc., ISBN 0-471-29340-7, New York, 530 pp.
- Borghesi, A., Bussoletti, E., Colangeli, L., & de Blasi, C. 1985, Laboratory study of SiC submicron particles at IR wavelengths - A comparative analysis, *Astron. Astrophys.*, Vol. 153, No. 1, pp. 1-8
- B<sup>2</sup>FH = Burbidge, E. M., Burbidge, G. R., Fowler, W. A., & Hoyle, F. (1957). Synthesis of the Elements in Stars, *Rev. Mod. Phys.*, Vol. 29, p. 547
- Cameron, A. G. W. (1957). Nuclear Reactions in Stars and Nucleogenesis, *Publ. Astron. Soc. Pac.*, Vol. 69, p. 201
- Chan, S. J., & Kwok, S. (1990). Evolution of infrared carbon stars, *Astron. Astrophys.*, Vol. 237, p. 354
- Choyke, W. J., & Patrick, L. (1957). Absorption of Light in Alpha SiC near the Band Edge, *Phys. Rev.*, Vol. 105, p. 1721
- Choyke, W. J., & Patrick, L. (1968). Higher Absorption Edges in 6H SiC, *Phys. Rev.*, Vol. 172, No. 3, pp. 769-772
- Choyke, W. J., & Patrick, L. (1969). Higher Absorption Edges in Cubic SiC, *Phys. Rev.*, Vol. 187, No. 3, pp. 1041-1043
- Clayton, D. D., & Nittler, L. R. (2004). Astrophysics with Presolar Stardust, *Annu. Rev. Astron. Astr.*, Vol. 42, p. 39
- Clément, D., Mutschke, H., Klein, R., & Henning, Th. (2003). New Laboratory Spectra of Isolated  $\beta$ -SiC Nanoparticles: Comparison with Spectra Taken by the Infrared Space Observatory, *Astrophys. J.*, Vol. 594, No. 1, pp. 642-650
- Clube, K. L., & Gledhill, T. M. (2004). Mid-infrared imaging and modelling of the dust shell around post-AGB star HD 187885 (IRAS 19500-1709), *Mon. Not. R. Astron. Soc.*, Vol. 355, No. 3, pp. L17-L21
- Corman, A. B. (2010). Carbon Stars and Silicon Carbide, PhD thesis, University of Missouri-Columbia, USA
- Corman, A. B., Hofmeister, A. M., Speck, A. K., & Pitman, K. M. (2011). Optical Constants of Silicon Carbide. III. Shape Effects on Small Silicon Carbide Grains, *Astrophys. J.*, in preparation
- Daulton, T. L., Bernatowicz, T. J., Lewis, R. S., Messenger, S., Stadermann, F. J., & Amari, S. (2002). Polytype Distribution in Circumstellar Silicon Carbide, *Science*, Vol. 296, No. 5574, pp. 1852-1855
- Daulton, T. L., Bernatowicz, T. J., Lewis, R. S., Messenger, S., Stadermann, F. J., & Amari, S. (2003). Polytype distribution of circumstellar silicon carbide - microstructural

- characterization by transmission electron microscopy, *Geochim. Cosmochim. Ac.*, Vol. 67, No. 24, pp. 4743-4767
- de Graauw, T., et al. (1996). Observing with the ISO Short-Wavelength Spectrometer, *Astron. Astrophys.*, Vol. 315, pp. L49-L54
- Devaty, R. P., & Choyke, W. J. (1997). Optical Characterization of Silicon Carbide Polytypes, *Phys. Status Solidi (A), Applied Research*, Vol. 162, No. 1, pp. 5-38
- Ferguson, J. W., Alexander, D. R., Allard, F., Barman, T., Bodnarik, J. G., Hauschildt, P. H., Hefner-Wong, A., & Tamanai, A. (2005). Low-Temperature Opacities, *Astrophys. J.*, Vol. 623, No. 1, pp. 585-596
- Friedemann, C. (1969). Evolution of silicon carbide particles in the atmospheres of carbon stars, *Physica*, Vol. 41, p. 139
- Friedemann, C., Gürtler, J., Schmidt, R., & Dorschner, J. (1981). The 11.5 micrometer emission from carbon stars - Comparison with IR spectra of submicrometer-sized silicon carbide grains, *Astrophys. Space Sci.*, Vol. 79, No. 2, pp. 405-417
- Gavrilenko, V. I. (1995). Calculated differential reflectance of the (110) surface of cubic silicon carbide, *Appl. Phys. Lett.*, Vol. 67, pp. 16-18
- Gavrilenko, V. I., & Bechstedt, F. (1997). Optical functions of semiconductors beyond density-functional theory and random-phase approximation, *Phys. Rev. B*, Vol. 55, No. 7, pp. 4343-4352
- Gilman, R. C. (1969). On the Composition of Circumstellar Grains, *Astrophys. J.*, Vol. 155, p. L185
- Gilra, D. P. (1971). Composition of Interstellar Grains, *Nature*, Vol. 229, No. 5282, pp. 237-241
- Gilra, D.P. (1972). Collective Excitations in Small Solid Particles and Astronomical Applications, Ph.D. thesis, University of Wisconsin-Madison, Dissertation Abstracts International, Vol. 33-11, Sect. B, p. 5114
- Goebel, J. H., Cheeseman, P., & Gerbault, F. (1995). The 11 Micron Emissions of Carbon Stars, *Astrophys. J.*, Vol. 449, p. 246
- Griffin, I. P. (1990). A model for the infrared and radio spectral energy distribution of IRC + 10 deg 216, *Mon. Not. R. Astron. Soc.*, Vol. 247, pp. 591-605
- Griffin, I. P. (1993). A model for the circumstellar envelope of WX SER, *Mon. Not. R. Astron. Soc.*, Vol. 260, pp. 831-843
- Groenewegen, M. A. T. (1995). Dust shells around infrared carbon stars, *Astron. Astrophys.*, Vol. 293, pp. 463-478.
- Groenewegen, M. A. T., Whitelock, P. A., Smith, C. H., & Kerschbaum, F. (1998). Dust shells around carbon Mira variables, *Mon. Not. R. Astron. Soc.*, Vol. 293, p. 18
- Groenewegen, M. A. T., Sloan, G. C., Soszyński, I., & Petersen, E. A. (2009). Luminosities and mass-loss rates of SMC and LMC AGB stars and red supergiants, *Astron. Astrophys.*, Vol. 506, No. 3, pp. 1277-1296
- Gyngard, F. (2009). Isotopic studies of presolar silicon carbide and oxide grains as probes of nucleosynthesis and the chemical evolution of the galaxy, Ph.D. thesis (Proquest, AAT 3387342), Washington University in St. Louis, USA, 165 pp.
- Hackwell, J. A. (1972). Long wavelength spectrometry and photometry of M, S and C-stars, *Astron. Astrophys.*, Vol. 21, p. 239
- Heck, P. R. (2005) Helium and neon in presolar silicon carbide grains and in relict chromite grains from fossil meteorites and micrometeorites as tracers of their origin, Ph.D.

- thesis Proquest, AAT C821918), Eidgenoessische Technische Hochschule Zuerich (Switzerland), 155 pp.
- Heck, P. R., Pellin, M. J., Davis, A. M., Martin, I., Renaud, L., Benbalagh, R., Isheim, D., Seidman, D. N., Hiller, J., Stephan, T., Lewis, R. S., Savina, M. R., Mane, A., Elam, J., Stadermann, F. J., Zhao, X., Daulton, T. L., & Amari, S. (2010). Atom-Probe Tomographic Analyses of Presolar Silicon Carbide Grains and Meteoritic Nanodiamonds – First Results on Silicon Carbide, *41st Lunar Planet. Sci. Conf.*, March 1-5, 2010, The Woodlands, Texas, No. 1533, p. 2112
- Henkel, T., Stephan, T., Jessberger, E. K., Hoppe, P., Strelbel, R., Amari, S., & Lewis, R. S. (2007). 3-D elemental and isotopic composition of presolar silicon carbides, *Meteorit. Planet. Sci.*, Vol. 42, No. 7, pp. 1121-1134
- Henning, T. (2010). Laboratory Astrophysics of Cosmic Dust Analogues, In: *Lecture Notes in Physics 815 Astromineralogy* (2<sup>nd</sup> ed.), Th. Henning (ed.), pp. 313-329, Springer-Verlag, ISBN 978-3-642-13258-2, Berlin, Heidelberg
- Hoare, M. G. (1990). The dust content of two carbon-rich planetary nebulae, *Mon. Not. R. Astron. Soc.*, Vol. 244, pp. 193-206
- Hofmeister, A. M., Keppel, E., & Speck, A. K. (2003). Absorption and reflection infrared spectra of MgO and other diatomic compounds, *Mon. Not. R. Astron. Soc.*, Vol. 345, No. 1, pp. 16-38
- Hofmeister, A. M., Pitman, K. M., Goncharov, A. F., & Speck, A. K. (2009) Optical Constants of Silicon Carbide for Astrophysical Applications. II. Extending Optical Functions from Infrared to Ultraviolet Using Single-Crystal Absorption Spectra, *Astrophys. J.*, Vol. 696, No. 2, pp. 1502-1516
- Hoppe, P. (2009). Stardust in Meteorites and IDPs: Current Status, Recent Advances, and Future Prospects, In: *Cosmic Dust - Near and Far*, ASP Conference Series, Vol. 414, ed. Th. Henning, E. Grün, & J. Steinacker, p.148
- Hoppe, P., & Besmehn, A. (2002). Evidence for Extinct Vanadium-49 in Presolar Silicon Carbide Grains from Supernovae, *Astrophys. J.*, Vol. 576, No. 1, pp. L69-L72.
- Hoppe, P., & Ott, U. (1997). Mainstream silicon carbide grains from meteorites, In: *Astrophysical implications of the laboratory study of presolar materials*, AIP Conference Proceedings, Vol. 402, pp. 27-58
- Hoppe, P., & Zinner, E. (2000). Presolar dust grains from meteorites and their stellar sources, *J. Geophys. Res.*, Vol. 105, No. A5, pp. 10371-10386
- Hoppe, P., Amari, S., Zinner, E., Ireland, T., & Lewis, R. S. (1994a). Carbon, nitrogen, magnesium, silicon, and titanium isotopic compositions of single interstellar silicon carbide grains from the Murchison carbonaceous chondrite, *Astrophys. J.*, Vol. 430, No. 2, pp. 870-890
- Hoppe, P., Pungitore, B., Eberhardt, P., Amari, S., & Lewis, R. S. (1994b) Ion imaging of small interstellar grains, *Meteoritics*, Vol. 29, No. 4, pp. 474-475
- Hoppe, P., Strelbel, R., Eberhardt, P., Amari, S., & Lewis, R. S. (1996) Small SiC grains and a nitride grain of circumstellar origin from the Murchison meteorite: Implications for stellar evolution and nucleosynthesis, *Geochim. Cosmochim. Ac.*, Vol. 60, No. 5, pp. 883-907
- Hoppe, P., Strelbel, R., Eberhardt, P., Amari, S., & Lewis, R. S. (2000) Isotopic properties of silicon carbide X grains from the Murchison meteorite in the size range 0.5-1.5  $\mu\text{m}$ , *Meteorit. Planet. Sci.*, Vol. 35, No. 6, pp. 1157-1176

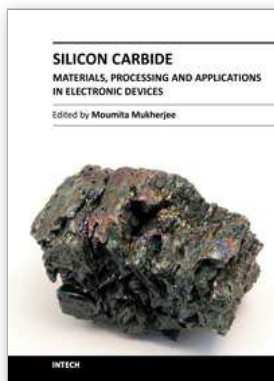
- Hoppe, P., Lodders, K., Strebler, R., Amari, S., & Lewis, R. S. (2001). Boron in Presolar Silicon Carbide Grains from Supernovae, *Astrophys. J.*, Vol. 551, No. 1, pp. 478-485
- Huffman, D. R. (1988). Methods and Difficulties in Laboratory Studies of Cosmic Dust Analogues, In: *Experiments on Cosmic Dust Analogues*, eds. E. Bussoletti, C. Fusco, & G. Longo, Astrophysics and Space Science Library, Vol. 149, p. 25, Kluwer Academic Publishers, Dordrecht.
- Iben, I., Jr., & Renzini, A. (1983). Asymptotic giant branch evolution and beyond, in: Annual review of Astron. Astrophys.. Vol. 21 (Palo Alto, CA, Annual Reviews, Inc.), pp. 271-342
- Ismail, A. M., & Abu-Safia, H. (2002). Calculated and measured reflectivity of some p-type SiC polytypes, *J. Appl. Phys.*, Vol. 91, No. 7, pp. 4114-4116
- Jennings, C. L., Savina, M. R., Messenger, S., Amari, S., Nichols, R. H., Jr., Pellin, M. J., & Podosek, F. A., (2002). Indarch SiC by TIMS, RIMS, and NanoSIMS, *33rd Lunar Planet. Sci. Conf.*, March 11-15, 2002, Houston, Texas, abstract no. 1833
- Jiang, B. W., Zhang, K., & Li, A. (2005). On Silicon Carbide Grains as the Carrier of the 21  $\mu\text{m}$  Emission Feature in Post-Asymptotic Giant Branch Stars, *Astrophys. J.*, Vol. 630, No. 1, pp. L77-L80
- Kessler, M. F., Steinz, J. A.; Anderegg, M. E.; Clavel, J.; Drechsel, G.; Estaria, P.; Faelker, J.; Riedinger, J. R.; Robson, A.; Taylor, B. G.; Ximénez de Ferrán, S. (1996). The Infrared Space Observatory (ISO) mission, *Astron. Astrophys.*, Vol. 315, No. 2, pp. L27 - L31
- Kimura, Y., Nuth, J. A., III, & Ferguson, F. T. (2005a). Is the 21 Micron Feature Observed in Some Post-AGB Stars Caused by the Interaction between Ti Atoms and Fullerenes? *Astrophys. J.*, Vol. 632, No. 2, pp. L159-L162
- Kimura, Y., Ishikawa, M., Kurumada, M., Tanigaki, T., Suzuki, H., & Kaito, C. (2005b). Crystal structure and growth of carbon-silicon mixture film prepared by ion sputtering, *Journal of Crystal Growth*, Vol. 275, pp. e977-e981
- Kozasa, T., Dorschner, J., Henning, Th., & Stognienko, R. (1996). Formation of SiC grains and the 11.3 $\mu\text{m}$  feature in circumstellar envelopes of carbon stars, *Astron. Astrophys.*, Vol. 307, pp. 551-560
- Kwok, S., Volk, K. M., & Hrivnak, B. J. (1989). A 21 micron emission feature in four protoplanetary nebulae, *Astrophys. J. Lett.*, Vol. 345, pp. L51-L54
- Ladjal, D., Justtanont, K., Groenewegen, M. A. T., Blommaert, J. A. D. L., Waelkens, C., & Barlow, M. J. (2010). 870  $\mu\text{m}$  observations of evolved stars with LABOCA, *Astron. Astrophys.*, Vol. 513, p. A53
- Lambrecht, W. R. L., Segall, B., Suttrop, W., Yoganathan, M., Devaty, R. P., Choyke, W. J., Edmond, J. A., Powell, J. A., & Alouani, M. (1993). Optical reflectivity of 3C and 4H-SiC polytypes: Theory and experiment, *Appl. Phys. Lett.*, Vol. 63, pp. 2747- 2749
- Lambrecht, W. R. L., Segall, B., Yoganathan, M., Suttrop, W., Devaty, R. P., Choyke, W. J., Edmond, J. A., Powell, J. A., & Alouani, M. (1994). Calculated and measured uv reflectivity of SiC polytypes, *Phys. Rev. B*, Vol. 50, pp. 10722-10726
- Lambrecht, W. R. L., Limpijumnong, S., Rashkeev, S. N., & Segall, B. (1997). Electronic Band Structure of SiC Polytypes: A Discussion of Theory and Experiment, *Phys. Status Solidi (B)*, *Applied Research*, Vol. 202, No. 1, pp. 5-33
- Laor, A., & Draine, B. T. (1993). Spectroscopic constraints on the properties of dust in active galactic nuclei, *Astrophys. J.*, Vol. 402, No. 2, pp. 441-468

- Lindquist, O. P. A., Schubert, M., Arwin, H., & Jarrendahl, K. (2004). Infrared to vacuum ultraviolet optical properties of 3C, 4H and 6H silicon carbide measured by spectroscopic ellipsometry, *Thin Solid Films*, Vol. 455-456, pp. 235-238
- Little-Marenin, I. R. (1986). Carbon stars with silicate dust in their circumstellar shells, *Astrophys. J. Lett.*, Vol. 307, pp. L15-L19
- Logothetidis, S., & Petalas, J. (1996). Dielectric function and reflectivity of 3C-silicon carbide and the component perpendicular to the c axis of 6H-silicon carbide in the energy region 1.5-9.5 eV, *J. Appl. Phys.*, Vol. 80, pp. 1768- 1772
- Lorenz-Martins, S., & Lefevre, J. (1993). SiC in circumstellar shells around C stars, *Astron. Astrophys.*, Vol. 280, pp. 567-580
- Lorenz-Martins, S., & Lefevre, J. (1994). SiC grains and evolution of carbon stars, *Astron. Astrophys.*, Vol. 291, pp. 831-841
- Lorenz-Martins, S., de Araújo, F. X., Codina Landaberry, S. J., de Almeida, W. G., & de Nader, R. V. (2001). Modeling of C stars with core/mantle grains: Amorphous carbon + SiC, *Astron. Astrophys.*, Vol. 367, pp. 189-198
- Lubinsky, A. R., Ellis, D. E., & Painter, G. S. (1975). Electronic structure and optical properties of 3C-SiC, *Phys. Rev. B*, Vol. 11, p. 1537
- Martin, P. G., & Rogers, C. (1987). Carbon grains in the envelope of IRC +10216, *Astrophys. J.*, Vol. 322, pp. 374-392
- Mauron, N., & Huggins, P. J. (2006). Imaging the circumstellar envelopes of AGB stars, *Astron. Astrophys.*, Vol. 452, pp. 257-268
- Min, M., Hovenier, J. W., & de Koter, A. (2003). Shape effects in scattering and absorption by randomly oriented particles small compared to the wavelength, *Astron. Astrophys.*, Vol. 404, pp. 35-46
- Mutschke, H., Andersen, A. C., Clément, D., Henning, Th., & Peiter, G. (1999). Infrared properties of SiC particles, *Astron. Astrophys.*, Vol. 345, pp. 187-202
- Nakashima, S., & Harima, H. (1997). Raman Investigation of SiC Polytypes, *Physica Status Solidi A - Applied Research*, Vol. 162, p. 39
- Nenkova, M., Ivezić, Z., & Elitzur, M. (2000). *Thermal Emission Spectroscopy and Analysis of Dust, Disks, and Regoliths*, Vol. 196, p. 77
- Neugebauer, G., Soifer, B. T., Beichman, C. A., Aumann, H. H., Chester, T. J., Gautier, T. N., Lonsdale, C. J., Gillett, F. C., Hauser, M. G., & Houck, J. R. (1984). Early results from the Infrared Astronomical Satellite, *Science*, Vol. 224, pp. 14-21
- Nichols, R. H. (1992). The origin of neon-E: Neon-E in single interstellar silicon carbide and graphite grains, Ph.D. thesis, Washington Univ., Seattle, USA
- Nicolussi, G. K., Davis, A. M., Pellin, M. J., Lewis, R. S., Clayton, R. N., & Amari, S. (1997). S-process zirconium in individual presolar silicon carbide grains, *Lunar Planet. Sci.*, Vol. 28, p. 23
- Nicolussi, G. K., Pellin, M. J., Lewis, R. S., Davis, A. M., Amari, S., & Clayton, R. N. (1998). Molybdenum Isotopic Composition of Individual Presolar Silicon Carbide Grains from the Murchison Meteorite, *Geochim. Cosmochim. Ac.*, Vol. 62, pp. 1093-1104
- Ninomiya, S., & Adachi, S. (1994). Optical Constants of 6H SiC Single Crystals, *Jpn. J. Appl. Phys.*, Vol. 33, No. 5A, pp. 2479
- Obarich, V. A. (1971). Optical constants of  $\alpha$ -SiC(6H) in the intrinsic absorption region, *J. Appl. Spectrosc.*, Vol. 15, No. 1, pp. 959-961

- Orofino, V., Blanco, A., Mennella, V., Bussoletti, E., Colangeli, L., & Fonti, S. (1991). Experimental extinction properties of granular mixtures of silicon carbide and amorphous carbon, *Astron. Astrophys.*, Vol. 252, No. 1, pp. 315-319
- Ott, U. (2010). The Most Primitive Material in Meteorites, In: *Lecture Notes in Physics 815 Astromineralogy (2<sup>nd</sup> ed.)*, ed. Th. Henning, pp. 277-311, Springer-Verlag, ISBN 978-3-642-13258-2, Berlin, Heidelberg
- Ott, U., & Merchel, S. (2000). Noble Gases and the Not So Unusual Size of Presolar SiC in Murchison, *31<sup>st</sup> Lunar Planet. Sci. Conf.*, March 13-17, 2000, Houston, Texas, abstract no. 1356
- Papoular, R., Cauchetier, M., Begin, S., & Lecaer, G. (1998). Silicon carbide and the 11.3- $\mu\text{m}$  feature, *Astron. Astrophys.*, Vol. 329, pp. 1035-1044
- Pégourié, B. (1988). Optical properties of alpha silicon carbide, *Astron. Astrophys.*, Vol. 194, No. 1-2, pp. 335-339
- Petalas, J., Logothetidis, S., Gioti, M., & Janowitz, C. (1998). Optical Properties and Temperature Dependence of the Interband Transitions of 3C- and 6H-SiC in the Energy Region 5 to 10 eV, *Phys. Status Solidi (B)*, Vol. 209, No. 2, pp. 499-521
- Philipp, H. R. (1958). Intrinsic Optical Absorption in Single-Crystal Silicon Carbide, *Phys. Rev.*, Vol. 111, pp. 440
- Philipp, H. R., & Taft, E. A. (1960). Intrinsic Optical Absorption in Single Crystal Silicon Carbide, In: *Silicon Carbide*, ed. J. R. O'Connor & J. Smiltens, pp. 366-370, Pergamon, New York
- Pitman, K. M., Hofmeister, A. M., Corman, A. B., & Speck, A. K. (2008). Optical properties of silicon carbide for astrophysical applications, I. New laboratory infrared reflectance spectra and optical constants, *Astron. Astrophys.*, Vol. 483, pp. 661-672
- Prombo, C. A., Podosek, F. A., Amari, S., & Lewis, R. S. (1993). S-process BA isotopic compositions in presolar SiC from the Murchison meteorite, *Astrophys. J.*, Vol. 410, No. 1, pp. 393-399
- Rehn, V., Stanford, J. L., Jones, V. O., & Choyke, W. J. (1976). *Proc. 13th Internat. Conf. Physics of Semiconductors*, Marves, Rome, 1976, p. 985
- Savina, M. R., Davis, A. M., Tripa, C. E., Pellin, M. J., Clayton, R. N., Lewis, R. S., Amari, S., Gallino, R., & Lugaro, M. (2003) Barium isotopes in individual presolar silicon carbide grains from the Murchison meteorite, *Geochim. Cosmochim. Ac.*, Vol. 67, No. 17, pp. 3201-3214
- Skrutskie, M. F., Reber, T. J., Murphy, N. W., & Weinberg, M. D. (2001). Inferring Milky Way Structure from 2MASS-selected Carbon Stars, *Bulletin of the American Astronomical Society*, Vol. 33, p. 1437
- Sloan, G. C., Little-Marenin, I. R., & Price, S. D. (1998). The carbon-rich dust sequence - Infrared spectral classification of carbon stars, *Astron. J.*, Vol. 115, p. 809
- Speck, A. K. (1998). The Mineralogy of Dust Around Evolved Stars, PhD thesis, University College London
- Speck, A. K., & Hofmeister, A. M. (2004). Processing of Presolar Grains around Post-Asymptotic Giant Branch Stars: Silicon Carbide as the Carrier of the 21 Micron Feature, *Astrophys. J.*, Vol. 600, No. 2, pp. 986-991
- Speck, A. K., Barlow, M. J., & Skinner, C. J. (1997). The nature of the silicon carbide in carbon star outflows, *Mon. Not. R. Astron. Soc.*, Vol. 288, p. 431

- Speck, A. K., Hofmeister, A. M., & Barlow, M. J. (1999). The SiC Problem: Astronomical and Meteoritic Evidence, *Astrophys. J.*, Vol. 513, No. 1, pp. L87-L90
- Speck, A. K., Thompson, G. D., & Hofmeister, A. M. (2005). The Effect of Stellar Evolution on SiC Dust Grain Sizes, *Astrophys. J.*, Vol. 634, pp. 426-435
- Speck, A. K., Cami, J., Markwick-Kemper, C., Leisenring, J., Szczerba, R., Dijkstra, C., Van Dyk, S., & Meixner, M. (2006). The Unusual Spitzer Spectrum of the Carbon Star IRAS 04496-6958: A Different Condensation Sequence in the LMC?, *Astrophys. J.*, Vol. 650, pp. 892-900
- Speck, A. K., Corman, A. B., Wakeman, K., Wheeler, C. H., & Thompson, G. (2009). Silicon Carbide Absorption Features: Dust Formation in the Outflows of Extreme Carbon Stars, *Astrophys. J.*, Vol. 691, pp. 1202-1221
- Spitzer, W. G., Kleinman, D., & Frosch, C. J. (1959a). Infrared Properties of Cubic Silicon Carbide Films, *Phys. Rev.*, Vol. 113, pp. 133-136
- Spitzer, W. G., Kleinman, D., & Walsh, D. (1959b). Infrared Properties of Hexagonal Silicon Carbide, *Phys. Rev.*, Vol. 113, pp. 127-132
- Srinivasan, S., Sargent, B. A., Matsuura, M., Meixner, M., Kemper, F., Tielens, A. G. G. M., Volk, K., Speck, A. K., Woods, P. M., Gordon, K., Marengo, M., & Sloan, G. C. (2010). The mass-loss return from evolved stars to the Large Magellanic Cloud. III. Dust properties for carbon-rich asymptotic giant branch stars, *Astron. Astrophys.*, Vol. 524, p. A49
- Steffen, M., Szczerba, R., Menshchikov, A., & Schoenberner, D. (1997). Hydrodynamical models and synthetic spectra of circumstellar dust shells around AGB stars, *Astron. Astrophys.*, Vol. 126, pp. 39-65
- Stephens, J.R. (1980). Visible and ultraviolet (800-130 nm) extinction of vapor-condensed silicate, carbon, and silicon carbide smokes and the interstellar extinction curve, *Astrophys. J.*, Vol. 237, pp. 450-461
- Stroud, R. M., Nittler, L. R., & Hoppe, P. (2004). Microstructures and Isotopic Compositions of Two SiC X Grains, *Meteorit. Planet. Sci.*, Vol. 39, p. 5039
- Theodorou, G., Tsegas, G., & Kaxiras, E. (1999). Theory of electronic and optical properties of 3C-SiC, *J. Appl. Phys.*, Vol. 85, No. 4, pp. 2179-2184
- Thompson, G. D., Corman, A. B., Speck, A. K., & Dijkstra, C. (2006). Challenging the Carbon Star Dust Condensation Sequence: Anarchist C Stars, *Astrophys. J.*, Vol. 652, p. 1654
- Treffers, R., & Cohen, M. (1974). High-resolution spectra of cool stars in the 10- and 20-micron regions, *Astrophys. J.*, Vol. 188, p. 545
- Ueta, T., & Meixner, M. (2003). 2-DUST: A Dust Radiative Transfer Code for an Axisymmetric System, *Astrophys. J.*, Vol. 586, No. 2, pp. 1338-1355
- Van Schmus, W. R., & Wood, J. A. (1967). A chemical-petrologic classification for the chondritic meteorites, *Geochim. Cosmochim. Ac.*, Vol. 31, pp. 747-765
- Volk, K., Kwok, S., & Langill, P. P. (1992). Candidates for extreme carbon stars, *Astrophys. J.*, Vol. 391, p. 285
- Volk, K., Kwok, S., & Hrivnak, B. J. (1999). High-Resolution Infrared Space Observatory Spectroscopy of the Unidentified 21 Micron Feature, *Astrophys. J.*, Vol. 516, No. 2, pp. L99-L102
- Volk, K., Xiong, G., & Kwok, S. (2000). Infrared Space Observatory Spectroscopy of Extreme Carbon Stars, *Astrophys. J.*, Vol. 530, p. 408

- Wheeler, B. (1966). The ultraviolet reflectivity of  $\alpha$  and  $\beta$  SiC, *Solid State Commun.*, Vol. 4, No. 4, pp. 173-175.
- Willacy, K., & Cherchneff, I. (1998). Silicon and sulphur chemistry in the inner wind of IRC+10216, *Astron. Astrophys.*, Vol. 330, p. 676
- Willems, F. J. (1988). IRAS low-resolution spectra of cool carbon stars. II – Stars with thin circumstellar shells. III – Stars with thick circumstellar shells, *Astron. Astrophys.*, Vol. 203, pp. 51-70
- Windsteig, W., Dorfi, E. A., Hoefner, S., Hron, J., & Kerschbaum, F. (1997). Mid- and far-infrared properties of dynamical models of carbon-rich long-period variables, *Astron. Astrophys.*, Vol. 324, pp. 617-623
- Xie, C., Xu, P., Xu, F., Pan, H., & Li, Y. (2003). First-principles studies of the electronic and optical properties of 6H-SiC, *Physica B*, Vol. 336, pp. 284-289
- Yin, Q.-Z., Lee, C.-T. A., & Ott, U. (2006). Signatures of the s-process in presolar silicon carbide grains: Barium through hafnium, *Astrophys. J.*, Vol. 647, pp. 676-684



## Silicon Carbide - Materials, Processing and Applications in Electronic Devices

Edited by Dr. Moumita Mukherjee

ISBN 978-953-307-968-4

Hard cover, 546 pages

**Publisher** InTech

**Published online** 10, October, 2011

**Published in print edition** October, 2011

Silicon Carbide (SiC) and its polytypes, used primarily for grinding and high temperature ceramics, have been a part of human civilization for a long time. The inherent ability of SiC devices to operate with higher efficiency and lower environmental footprint than silicon-based devices at high temperatures and under high voltages pushes SiC on the verge of becoming the material of choice for high power electronics and optoelectronics. What is more important, SiC is emerging to become a template for graphene fabrication, and a material for the next generation of sub-32nm semiconductor devices. It is thus increasingly clear that SiC electronic systems will dominate the new energy and transport technologies of the 21st century. In 21 chapters of the book, special emphasis has been placed on the "materials" aspects and developments thereof. To that end, about 70% of the book addresses the theory, crystal growth, defects, surface and interface properties, characterization, and processing issues pertaining to SiC. The remaining 30% of the book covers the electronic device aspects of this material. Overall, this book will be valuable as a reference for SiC researchers for a few years to come. This book prestigiously covers our current understanding of SiC as a semiconductor material in electronics. The primary target for the book includes students, researchers, material and chemical engineers, semiconductor manufacturers and professionals who are interested in silicon carbide and its continuing progression.

### How to reference

In order to correctly reference this scholarly work, feel free to copy and paste the following:

Karly M. Pitman, Angela K. Speck, Anne M. Hofmeister and Adrian B. Corman (2011). Optical Properties and Applications of Silicon Carbide in Astrophysics, Silicon Carbide - Materials, Processing and Applications in Electronic Devices, Dr. Moumita Mukherjee (Ed.), ISBN: 978-953-307-968-4, InTech, Available from: <http://www.intechopen.com/books/silicon-carbide-materials-processing-and-applications-in-electronic-devices/optical-properties-and-applications-of-silicon-carbide-in-astrophysics>

# INTECH

open science | open minds

### InTech Europe

University Campus STeP Ri  
Slavka Krautzeka 83/A  
51000 Rijeka, Croatia  
Phone: +385 (51) 770 447

### InTech China

Unit 405, Office Block, Hotel Equatorial Shanghai  
No.65, Yan An Road (West), Shanghai, 200040, China  
中国上海市延安西路65号上海国际贵都大饭店办公楼405单元  
Phone: +86-21-62489820

Fax: +385 (51) 686 166  
www.intechopen.com

Fax: +86-21-62489821

© 2011 The Author(s). Licensee IntechOpen. This is an open access article distributed under the terms of the [Creative Commons Attribution 3.0 License](#), which permits unrestricted use, distribution, and reproduction in any medium, provided the original work is properly cited.